CVR-2007-178R1

Online Data Supplement

Calsequestrin Mutation and Catecholaminergic Polymorphic Ventricular Tachycardia: A Simulation Study of Cellular Mechanism

by
Gregory M. Faber[1] and Yoram Rudy[2]

Department of Biomedical Engineering, Case Western Reserve University[1], Cleveland, OH 44106-7207
Cardiac Bioelectricity and Arrhythmia Center and Department of Biomedical Engineering, Washington University[2], St. Louis, MO 63130-4899

Running Title:

CASQ2 Mutation and Spontaneous Calcium Release

Word Count:

N/A

Address correspondence and reprint requests to:
Yoram Rudy, Director
Cardiac Bioelectricity and Arrhythmia Center
290 Whitaker Hall
Campus Box 1097,
One Brookings Drive,
St. Louis, MO 63130-4899, USA
Tel: (314) 935-8160
Fax: (314) 935-8168
Email: rudy@wustl.edu

DEFINITIONS AND ABBREVIATIONS

AP	Action potential
APD_{90}	Action potential duration measured at 90% repolarization
CL	Cycle length
RMP	Resting membrane potential
$Ca_V1.2$	L-type Ca^{2+} channel
RyR	Ryanodine receptor SR Ca^{2+} release channel
CaT	Calcium transient
CICR	Calcium-induced calcium release
SOICR	Store-over-load induced calcium release
ISO	Isoproterenol
MOT	Mean Open Time
VDI	Voltage dependent inactivation
CDI	Calcium dependent inactivation
$ModeV$	L-type Ca^{2+} channel states in VDI gating mode
$ModeCa$	L-type Ca^{2+} channel states in CDI gating mode
f_{Ca}	CDI gate
$Mode0$	L-type Ca^{2+} channel states in a non-conducting mode
f_{M0}	Mode0 gate
$CASQ2$	Calsequestrin, Ca^{2+} buffer in JSR
$TRPN$	Troponin, Ca^{2+} buffer in myoplasm
$CMDN$	Calmodulin, Ca^{2+} buffer in myoplasm
SR	Sarcoplasmic reticulum
JSR	Junctional SR
NSR	Network SR
ss	Subspace
myo	Myoplasm
$I_{Ca(L)}$	Ca^{2+} Current through L-type Ca^{2+} channel, μA/μF
$I_{Ca,Na}$	Na^{+} Current through L-type Ca^{2+} channel, μA/μF
$I_{Ca,K}$	K^{+} Current through L-type Ca^{2+} channel, μA/μF
I_{Na}	Fast Na^{+} Current, μA/μF
$I_{Na,b}$	Background Na^{+} Current, μA/μF
$I_{Ca,b}$	Background Ca^{2+} Current, μA/μF
$I_{Ca(T)}$	T-Type Ca^{2+} Current, μA/μF

I_{Kr}	Rapid delayed rectifier K^+ current, μA/μF
I_{Ks}	Slow delayed rectifier K^+ current, μA/μF
I_{K1}	Time independent K^+ current, μA/μF
I_{Kp}	Plateau K^+ Current, μA/μF
I_{NaCa}	Na^+-Ca^{2+} Exchanger in myoplasm, μA/μF
$I_{NaCa,ss}$	Na^+-Ca^{2+} Exchanger in subspace, μA/μF
I_{NaK}	Sodium-Potassium Pump, μA/μF
$I_{p,Ca}$	Sarcolemmal Ca^{2+} Pump, μA/μF
I_{rel}	Ca^{2+} release from JSR to subspace, mM/ms
I_{up}	Ca^{2+} uptake from myoplasm to SR, mM/ms
I_{leak}	Ca^{2+} leak from NSR to myoplasm, mM/ms
I_{tr}	Ca^{2+} transfer from NSR to JSR, mM/ms
I_{diff}	Ca^{2+} transfer from subspace to myoplasm, mM/ms
P_s	Membrane permeability to ion S, cm/s
$\overline{I_x}$	Maximum current carried through channel x, μA/μF
V_m	Transmembrane potential, mV
z_s	Valence of ion S
E_x	Reversal potential of current x, mV
$[S]_o$	Extracellular concentration of ion S, mM
$[S]_i$	Intracellular concentration of ion S, mM
$[S]_{ss}$	Subspace concentration of ion S, mM
$[Ca^{2+}]_{JSR}$	Ca^{2+} concentration in JSR (unbound Ca^{2+}), mM
$[Ca^{2+}]_{NSR}$	Ca^{2+} concentration in NSR, mM
Mito	Mitochondria
$[Ca^{2+}]_m$	Ca^{2+} concentration within the mitochondria, mM
β_{mito}	Free vs. total Ca^{2+} concentration ratio within the mitochondria
ρ_{mito}	Volume ratio between mitochondria and cytosol
k_{in}	Maximum rate of Ca^{2+} influx into mitochondria, mM/ms
k_{out}	Maximum rate of Ca^{2+} efflux into mitochondria, ms^{-1}
K_{mMito}	Half-saturation for Ca^{2+} uptake into mitochondria, μM

J_{inMito}	Ca^{2+} flux into mitochondria, mM/ms
$J_{outMito}$	Ca^{2+} flux out of mitochondria, mM/ms

ADDITIONAL METHODS

Simulation of Isoproterenol (ISO) Effects

In addition to its effects on $Ca_V1.2$, ISO also affects several other channels. In our simulations we include the effects of a saturating concentration of ISO (≥0.1 μM) on the slow delayed rectifier K^+ current (I_{Ks}), the Na^+-K^+ pump (I_{NaK}), the inwardly rectifying K^+ current (I_{K1}), and the SR Ca^{2+} ATPase (I_{up}). The increase in I_{Ks} magnitude following β-adrenergic stimulation has been well established [1, 2] with Bosch et al. [3] observing an 80% increase in current amplitude compared to control in the presence of 0.1 μM ISO. The magnitude of I_{NaK} has been observed to increase in the presence of cAMP-increasing drugs; 133% of control in guinea pig ventricular myocytes in the presence of 4 μM forskolin [4] and 140% of control in rat ventricular myocytes in the presence of 1 μM isoproterenol [5]. In this study, we increase I_{NaK} conservatively by 30%. The effect of isoproterenol on I_{K1} is a reduction of the inward rectification of the current [6, 7], which reduces the current magnitude at hyperpolarized potentials. We include this effect on I_{K1} as detailed in the **Equations**. In a study in mice ventricular myocytes, Li et al. [8] observed a 30% decrease in the time constant of relaxation of the CaT in the presence of 1 μM ISO and in a study by Chaudhri et al. [9] in rabbit ventricular myocytes, a 30% decrease in the time to 50% relaxation (RT_{50}) of the CaT was observed in the presence of 1 μM ISO. We increase I_{up} by 20% and achieve a 20% decrease in the time constant of relaxation of the CaT and a 20% decrease in the RT_{50} of the CaT at CL = 1500 ms. The modifications to the model equations reflecting these effects of ISO are detailed in the **Equations**.

Store-Overload-Induced Ca^{2+} Release (SOICR)

We modify the RyR model to allow for SOICR. The formulation is a function of the concentration of free Ca^{2+} in the junctional SR ($[Ca^{2+}]_{JSR}$) as proposed by Jiang et al. [10]. It should be noted that in this formulation (see **Equations**) the time constant associated with the SOICR function ($soicr_\tau$) is not a determinant of the frequency of spontaneous release but instead defines the duration of the spontaneous release event. Without this time constant, when $[Ca^{2+}]_{JSR}$ reaches the threshold for spontaneous release, a small amount of Ca^{2+} will be released and then $[Ca^{2+}]_{JSR}$ will drop below the threshold, terminating release. This is not observed experimentally; instead the initiation of a SR release event leads to a larger, more unified release of SR Ca^{2+} through communication between diadic spaces via Ca^{2+} waves [11, 12]. For the purpose of this study, this process is represented at a macroscopic level by $soicr_\tau$. This representation is successful in generating SOICR events that result in DADs with amplitude and duration similar to those observed experimentally [13-16]. The incidence and frequency of SOCIR events is a function of the total cellular Ca^{2+}, the rate of SR Ca^{2+} uptake, the rate of SR Ca^{2+} leak, and the amount of CASQ2 available to bind Ca^{2+}.

Although we utilize elevated luminal Ca^{2+} as the indicator for the initiation of SOICR, it is possible that the initiation SOICR occurs due to increased RyR opening as a result of elevated cytoplasmic Ca^{2+}. Following the application of ISO, we observe an increase in both peak and diastolic $[Ca^{2+}]_i$. Satoh et al. [17] observed increased occurrence of sparks in rabbit myocytes when diastolic $[Ca^{2+}]_i$ was elevated. Our model recreates $I_{Ca(L)}$, I_{rel}, and $[Ca^{2+}]_i$ that corresponds well to experimentally measured data at a variety of test potentials and pacing rates (see Faber et al. [18]). However, the model is

not formulated to reproduce properties of the cell at the microscopic level of spark formation. For this reason, we cannot investigate a possible mechanism of the initiation of SOICR due to stochastic openings of RyR channels as a result of elevated diastolic Ca^{2+}.

CASQ2 Mutation

We model the effects of the CASQ2 mutation D307H associated with CPVT in homozygous carriers as a reduction in total Ca^{2+} binding capacity of CASQ2. In a study by Viatchenko-Karpinski et al. [19], rat ventricular myocytes expressing $CASQ2^{D307H}$ via adenoviral gene transfer exhibited caffeine induced Ca^{2+} fluorescence signals which had amplitude 41% of control. A similar reduction in the amplitude of CaT fluorescence signals was observed during square voltage pulses from -50 mV to 0 mV applied for 400 ms every minute. In accordance with these experiments, in our simulations we assume a 60% reduction in CASQ2 binding capabilities for $CASQ2^{D307H}$. For the same pulse protocol as the experiment, we observe a CaT amplitude generated by the mutant $CASQ2^{D307H}$ that is 41% of control (data not shown). Changes to the model equations reflecting the CASQ2 mutation are provided in the Equations.

Ca^{2+} Uptake and Release by Mitochondria

We incorporated mitochondrial uptake and release of Ca^{2+} in the LRd model based upon the formulations of Roux and Marhl [20]. Modifications were made to their formulation to account for temperature differences (23°C in the experiment versus 37°C in our model) and for the larger concentration of mitochondria in ventricular myocytes

[21]. The addition of mitochondrial Ca^{2+} sequestration resulted in a slight decrease in CaT amplitude and diastolic $[Ca^{2+}]_i$, with the simulated contribution of mitochondria to relaxation of the CaT comparable to that measured experimentally [22].

Simulation Protocols

During pacing, a stimulus of -80 μA/μF is applied for a duration of 0.5 ms. The model is paced with a conservative current stimulus carried by K^+ [23]. A discrete time step of 0.0002 ms is used during computation of the AP (or during voltage clamp simulations) and 0.002 ms during the diastolic interval. APD is measured as the interval between the time of maximum upstroke velocity (dV/dt_{max}) and 90% repolarization (APD_{90}).

$Ca_V1.2$ State Residencies During an EAD

The process of EAD generation was shown previously in both simulations [24] and experiments [13, 25]. The Markov model of $Ca_V1.2$ permits us to explore the mechanism of EAD generation at the level of channel kinetic states. In Supplement Fig. 3A, we show the state residencies of $Ca_V1.2$ during the pause-induced EAD. Due to prolongation of the AP, channels which have inactivated (ModeCa and I_{Vs}) are able to recover and return to the Open state (O), which leads to increased $I_{Ca(L)}$ current and depolarization of the membrane potential. The membrane depolarization causes channels which have deactivated to reactivate (Closed channels (C_0+C_1+C_2+C_3) return to the Open state), which leads to increase of $I_{Ca(L)}$ and further elevation of the membrane potential. This positive-feedback between channel reactivation and membrane depolarization (initiated by recovery of channels from inactivated states) leads to formation of the EAD.

APD prolongation is critical for EAD formation; it allows time for channels which have inactivated to recover. If recovery from inactivation is prevented (either recovery from CDI or recovery from VDI) the EAD is abolished (Supplement Fig. 3B and 3C, respectively). The times selected to freeze the channels in their respective inactivated states correspond to peak channel occupancy in these states. For channels inactivated via CDI, this time is early ($t = 1040$ ms; 30 ms from AP onset), with strong correlation to the time of peak CaT. For channels inactivated via VDI, this time is later in the AP ($t = 1165$; 155 ms from AP onset).

EQUATIONS

For a complete list of model equations, see Faber et al. [18]. Below are the full equations for the $Ca_V1.2$ model and those equations which were modified for the simulations in this paper.

Model Equations

A. $Ca_V1.2$ - L-type Ca^{2+} Channel - $I_{Ca(L)}$

$$\alpha = 0.925 \cdot \exp(V_m / 30)$$
$$\beta = 0.39 \cdot \exp(-V_m / 40)$$
$$\alpha_0 = 4 \cdot \alpha$$
$$\alpha_1 = 3 \cdot \alpha$$
$$\alpha_2 = 2 \cdot \alpha$$
$$\alpha_3 = \alpha$$
$$\beta_0 = \beta$$
$$\beta_1 = 2 \cdot \beta$$
$$\beta_2 = 3 \cdot \beta$$
$$\beta_3 = 4 \cdot \beta$$
$$\gamma_f = 0.245 \cdot \exp(V_m / 10)$$
$$\gamma_s = 0.005 \cdot \exp(-V_m / 40)$$
$$\phi_f = 0.02 \cdot \exp(V_m / 500)$$
$$\phi_s = 0.03 \cdot \exp(-V_m / 280)$$
$$\lambda_f = 0.035 \cdot \exp(-V_m / 300)$$
$$\lambda_s = 0.0011 \cdot \exp(V_m / 500)$$
$$\omega_f = \left(\beta_3 \cdot \lambda_f \cdot \gamma_f\right) / \left(\alpha_3 \cdot \phi_f\right)$$
$$\omega_s = \left(\beta_3 \cdot \lambda_s \cdot \gamma_s\right) / \left(\alpha_3 \cdot \phi_s\right)$$
$$\omega_{sf} = \left(\lambda_s \cdot \phi_f\right) / \lambda_f \; ; \omega_{fs} = \phi_s$$

$Ca_V1.2$ Differential Equations:

$$\frac{dC_0}{dt} = C_1 \cdot \beta_0 - C_0 \cdot \alpha_0$$
$$\frac{dC_1}{dt} = C_0 \cdot \alpha_0 + C_2 \cdot \beta_1 - C_1 \cdot \left(\alpha_1 + \beta_0\right)$$

$$\frac{dC_2}{dt} = C_1 \cdot \alpha_1 + C_3 \cdot \beta_2 - C_2 \cdot (\alpha_2 + \beta_1)$$
$$\frac{dC_3}{dt} = C_2 \cdot \alpha_2 + O \cdot \beta_3 + I_{Vf} \cdot \omega_f + I_{Vs} \cdot \omega_s - C_3 \cdot (\alpha_3 + \beta_2 + \gamma_f + \gamma_s)$$
$$\frac{dO}{dt} = C_3 \cdot \alpha_3 + I_{Vf} \cdot \lambda_f + I_{Vs} \cdot \lambda_s - O \cdot (\beta_3 + \phi_f + \phi_s)$$
$$\frac{dI_{Vf}}{dt} = C_3 \cdot \gamma_f + O \cdot \phi_f + I_{Vs} \cdot \omega_{sf} - I_{Vf} \cdot (\omega_f + \lambda_f + \omega_{fs})$$
$$\frac{dI_{Vs}}{dt} = C_3 \cdot \gamma_s + O \cdot \phi_s + I_{Vf} \cdot \omega_{fs} - I_{Vs} \cdot (\omega_s + \lambda_s + \omega_{sf})$$

Rate to Enter ModeCa:

$$\delta = \frac{4}{1 + 1/[Ca^{2+}]_{ss}}$$

Rate to Leave ModeCa:

$$\theta = 0.01$$

CDI Gate:

$$f_{Ca} = \frac{\theta}{\delta + \theta} - \left(\left(\frac{\theta}{\delta + \theta} - f_{Ca} \right) \cdot \exp \frac{-dt}{1/(\delta + \theta)} \right)$$

Rate to Enter Mode0:

$$M0_{on} = 0.0008$$

Rate to Leave Mode0:

$$M0_{off} = 0.00018$$

Mode0 Gate:

$$f_{M0} = \frac{M0_{off}}{M0_{on} + M0_{off}}$$

$Ca_V1.2$ Driving Force:

$$\bar{I}_{Ca} = P_{Ca} \cdot z_{Ca}^2 \cdot \frac{V_m \cdot F^2}{RT} \cdot \frac{\gamma_{Cai} \cdot [Ca^{2+}]_{ss} \cdot \exp((z_{Ca} \cdot V_m \cdot F)/(RT)) - \gamma_{Cao} \cdot [Ca^{2+}]_o}{\exp((z_{Ca} \cdot V_m \cdot F)/(RT)) - 1}$$

$$P_{Ca} = 0.006615;\ \gamma_{Cai} = 0.01;\ \gamma_{Cao} = 0.341$$

$$\bar{I}_{Ca,Na} = P_{Na} \cdot z_{Na} \cdot \frac{V_m \cdot F^2}{RT} \cdot \frac{\gamma_{Nai} \cdot [Na^{+}]_{ss} \cdot \exp((z_{Na} \cdot V_m \cdot F)/(RT)) - \gamma_{Nao} \cdot [Na^{+}]_o}{\exp((z_{Na} \cdot V_m \cdot F)/(RT)) - 1}$$

$$P_{Na} = 8.265 \times 10^{-6};\ \gamma_{Nai} = 0.75;\ \gamma_{Nao} = 0.75$$

$$\bar{I}_{Ca,K} = P_K \cdot z_K \cdot \frac{V_m \cdot F^2}{RT} \cdot \frac{\gamma_{Ki} \cdot [K^{+}]_{ss} \cdot \exp((z_K \cdot V_m \cdot F)/(RT)) - \gamma_{Ko} \cdot [K^{+}]_o}{\exp((z_K \cdot V_m \cdot F)/(RT)) - 1}$$

$$P_K = 2.363 \times 10^{-6};\ \gamma_{Ki} = 0.75;\ \gamma_{Ko} = 0.75$$

$Ca_V1.2$ Current:

$$I_{Ca(L)} = \bar{I}_{Ca} \cdot f_{Ca} \cdot f_{M0} \cdot O$$
$$I_{Ca,Na} = \bar{I}_{Ca,Na} \cdot f_{Ca} \cdot f_{M0} \cdot O$$
$$I_{Ca,K} = \bar{I}_{Ca,K} \cdot f_{Ca} \cdot f_{M0} \cdot O$$

B. I_{rel}

Store-Overload-Induced Ca^{2+} Release:

$$soicr_{ss} = \frac{25}{\left(1 + \exp\left(\frac{6.8 - [Ca^{2+}]_{JSR}}{0.001}\right)\right)}$$

$$soicr_{\tau} = 125$$

$$soicr = soicr_{ss} - (soicr_{ss} - soicr) \cdot \exp(-dt / soicr_{\tau})$$

$$G_{rel} = 250 \cdot \left(\frac{gradedrel}{vgainofrel} + soicr\right)$$

C. Ca^{2+} Uptake and Release by Mitochondria

$$\beta_{mito} = 0.0025$$
$$\rho_{mito} = 0.02$$
$$k_{in} = 8.6 \times 10^{-5}$$
$$k_{out} = 4.28 \times 10^{-3}$$

$$k_{mMito} = 1$$

$$J_{inMito} = k_{in} \cdot \frac{\left(1000 \cdot [Ca^{2+}]_i\right)^8}{K_{mMito}^8 + \left(1000 \cdot [Ca^{2+}]_i\right)^8}$$

$$J_{outMito} = k_{out} \cdot [Ca^{2+}]_m$$

$$d[Ca^{2+}]_m = dt \cdot \left(\beta_{Mito} / \rho_{Mito}\right) \cdot \left(J_{inMito} - J_{outMito}\right)$$
$$[Ca^{2+}]_m = [Ca^{2+}]_m + d[Ca^{2+}]_m$$

D. β-adrenergic Effects

a. $Ca_V1.2$

$$\phi_s = 0.014 \cdot \exp(-V_m / 20)$$
$$\lambda_f = 0.015 \cdot \exp(-V_m / 300)$$
$$\lambda_s = 0.0022 \cdot \exp(V_m / 500)$$

$$\delta = \frac{5}{1 + 1/[Ca^{2+}]_{ss}}$$

$$\theta = \frac{0.009}{1 + \exp\left(10000 \cdot [Ca^{2+}]_{ss} - 5\right)} + 0.001$$

$$M\emptyset_{on} = 0.0004$$

$$M\emptyset_{off} = 0.0004545$$

b. I_{Ks}

$$\overline{G}_{Ks} = 0.42434 \cdot \left(1 + \frac{0.6}{1 + (3.8 \times 10^{-5} / [Ca^{2+}]_i)^{1.4}}\right)$$

$$\tau_{xs1} = \frac{1}{\frac{7.19 \times 10^{-5} \cdot (V_m + 34)}{1 - \exp(-0.148 \cdot (V_m + 34))} + \frac{1.31 \times 10^{-4} \cdot (V_m + 34)}{\exp(0.0687 \cdot (V_m + 34)) - 1}}$$

c. I_{K1}

$$\beta_{K1} = 2 + \frac{0.49124 \cdot \exp(0.08032 \cdot (V_m - E_{K1} + 5.476)) + \exp(0.06175 \cdot (V_m - E_{K1} - 594.31))}{1 + \exp(-0.5143 \cdot (V_m - E_{K1} + 4.753))}$$

d. I_{NaK}

$\overline{G}_{NaK} = 2.6$

e. SR Fluxes

$\overline{I_{up}} = 0.02079$ mM/ms

E. Calsequestrin Mutation

$[\overline{csqn}] = 4$ mM

F. Initial Ionic Concentrations and Markov Model State Residencies

End diastolic steady-state values for the model paced at CL = 1000 ms.

$[Ca^{2+}]_i$	8.21×10^{-5} mM
$[Ca^{2+}]_{ss}$	6.72×10^{-5} mM
$[Ca^{2+}]_m$	2.5×10^{-3} mM
$[K^+]_i$	137.6 mM
$[K^+]_{ss}$	137.6 mM
$[Na^+]_i$	10.71 mM
$[Na^+]_{ss}$	10.71 mM
$[Ca^{2+}]_{NSR}$	2.553 mM
$[Ca^{2+}]_{JSR}$	2.479 mM
$[Ca^{2+}]_o$	1.8 mM
$[K^+]_o$	4.5 mM
$[Na^+]_o$	130 mM

L-type Ca^{2+} Channel

$C_0 = 0.948$
$C_1 = 0.052$
$C_2 = 0$
$C_3 = 0$
$O = 0$
$I_{Vf} = 0$
$I_{Vs} = 0$

RyR

$C_1 = 0.890$
$C_2 = 0.021$
$C_3 = 0.003$
$C_4 = 0.001$

$O = 0$
$I_1 = 0.082$
$I_2 = 0.002$
$I_3 = 0.001$
$I_4 = 0$
$I_5 = 0$

REFERENCES

[1] Bennett PB, Begenisich TB. Catecholamines modulate the delayed rectifying potassium current (IK) in guinea pig ventricular myocytes. Pflugers Arch 1987;410:217-9.

[2] Yazawa K, Kameyama M. Mechanism of receptor-mediated modulation of the delayed outward potassium current in guinea-pig ventricular myocytes. J Physiol 1990;421:135-50.

[3] Bosch RF, Schneck AC, Kiehn J, Zhang W, Hambrock A, Eigenberger BW et al. beta3-Adrenergic regulation of an ion channel in the heart-inhibition of the slow delayed rectifier potassium current I(Ks) in guinea pig ventricular myocytes. Cardiovasc Res 2002;56:393-403.

[4] Kockskamper J, Erlenkamp S, Glitsch HG. Activation of the cAMP-protein kinase A pathway facilitates Na+ translocation by the Na+-K+ pump in guinea-pig ventricular myocytes. J Physiol 2000;523:561-74.

[5] Dobretsov M, Hastings SL, Stimers JR. Na(+)-K+ pump cycle during beta-adrenergic stimulation of adult rat cardiac myocytes. J Physiol 1998;507:527-39.

[6] Koumi S, Sato R. On the mechanism of alpha 1-adrenergic modulation of the inwardly-rectifying potassium channel gating in the human heart. Nippon Ika Daigaku Zasshi 1996;63:165-8.

[7] Koumi S, Backer CL, Arentzen CE, Sato R. beta-Adrenergic modulation of the inwardly rectifying potassium channel in isolated human ventricular myocytes. Alteration in channel response to beta-adrenergic stimulation in failing human hearts. J Clin Invest 1995;96:2870-81.

[8] Li L, Desantiago J, Chu G, Kranias EG, Bers DM. Phosphorylation of phospholamban and troponin I in beta-adrenergic-induced acceleration of cardiac relaxation. Am J Physiol Heart Circ Physiol 2000;278:H769-79.

[9] Chaudhri B, Del Monte F, Hajjar RJ, Harding SE. Interaction between increased SERCA2a activity and beta -adrenoceptor stimulation in adult rabbit myocytes. Am J Physiol Heart Circ Physiol 2002;283:H2450-7.

[10] Jiang D, Xiao B, Yang D, Wang R, Choi P, Zhang L et al. RyR2 mutations linked to ventricular tachycardia and sudden death reduce the threshold for store-overload-induced Ca2+ release (SOICR). Proc Natl Acad Sci U S A 2004;101:13062-7.

[11] Lipp P, Hüser J, Pott L, Niggli E. Subcellular properties of triggered Ca2+ waves in isolated citrate-loaded guinea-pig atrial myocytes characterized by ratiometric confocal microscopy. J Physiol 1996;497:599-610.

[12] Subramanian S, Viatchenko-Karpinski S, Lukyanenko V, Györke S, Wiesner TF. Underlying mechanisms of symmetric calcium wave propagation in rat ventricular myocytes. Biophys J 2001;80:1-11.

[13] Priori SG, Corr PB. Mechanisms underlying early and delayed afterdepolarizations induced by catecholamines. Am J Physiol 1990;258:H1796-805.

[14] Mamas MA, Terrar DA. Inotropic actions of protein kinase C activation by phorbol dibutyrate in guinea-pig isolated ventricular myocytes. Exp Physiol 2001;86:561-70.

[15] Miura M, Ishide N, Oda H, Sakurai M, Shinozaki T, Takishima T. Spatial features of calcium transients during early and delayed afterdepolarizations. Am J Physiol 1993;265:H439-44.

[16] Schlotthauer K, Bers DM. Sarcoplasmic reticulum Ca(2+) release causes myocyte depolarization. Underlying mechanism and threshold for triggered action potentials. Circ Res 2000;87:774-80.

[17] Satoh H, Blatter LA, Bers DM. Effects of [Ca2+]i, SR Ca2+ load, and rest on Ca2+ spark frequency in ventricular myocytes. Am J Physiol 1997;272:H657-68.

[18] Faber GM, Silva J, Livshitz L, Rudy Y. Kinetic Properties of the Cardiac L-type Ca2+ Channel and its Role in Myocyte Electrophysiology: A Theoretical Investigation. Biophys J 2007;92:1522-43.

[19] Viatchenko-Karpinski S, Terentyev D, Györke I, Terentyeva R, Volpe P, Priori SG et al. Abnormal calcium signaling and sudden cardiac death associated with mutation of calsequestrin. Circ Res 2004;94:471-7.

[20] Roux E, Marhl M. Role of sarcoplasmic reticulum and mitochondria in Ca2+ removal in airway myocytes. Biophys J 2004;86:2583-95.

[21] Bers DM: **Excitation-Contraction Coupling and Cardiac Contractile Force**, 2nd Edition edn. Dordrecht, The Netherlands: Kluwer Academic Publishers; 2001.

[22] Bassani RA, Bassani JW, Bers DM. Mitochondrial and sarcolemmal Ca2+ transport reduce [Ca2+]i during caffeine contractures in rabbit cardiac myocytes. J Physiol 1992;453:591-608.

[23] Hund TJ, Kucera JP, Otani NF, Rudy Y. Ionic charge conservation and long-term steady state in the Luo-Rudy dynamic cell model. Biophys J 2001;81:3324-31.

[24] Zeng J, Rudy Y. Early afterdepolarizations in cardiac myocytes: mechanism and rate dependence. Biophys J 1995;68:949-64.

[25] January CT, Riddle JM. Early afterdepolarizations: mechanism of induction and block. A role for L-type Ca2+ current. Circ Res 1989;64:977-90.

FIGURE CAPTIONS

FIGURE E1 State residencies of the L-type Ca^{2+} channel during the time course of the action potential at CL = 500 ms in the absence of ISO (black curve) and in the presence of ISO (grey curve). For identification of the channel states, refer to Paper Fig. 1B.

FIGURE E2 Effect of CASQ2 buffering capacity on **(A)** peak $[Ca^{2+}]_i$, **(B)** free Ca^{2+} in the JSR, and **(C)** total Ca^{2+} in the SR ($[Ca^{2+}]_{JSR}$ + Ca^{2+} bound CASQ2). The model is paced for 5 minutes at CL = 1500 ms (black curves) and CL = 500 ms (grey curves) in the absence of ISO. CASQ2 buffering capacity of 10 corresponds to WT conditions and CASQ2 buffering capacity of 4 corresponds to a 60% reduction in buffering capacity as observed with the mutation $CASQ2^{D307H}$.

FIGURE E3 EAD generation is abolished by preventing $I_{Ca(L)}$ recovery from inactivation. **Panels A-C** (top to bottom): post-pause APs with corresponding $I_{Ca(L)}$, $Ca_V1.2$ closed-state residency (C_0+C_1+C_2+C_3), open-state residency (O), slow VDI state residency (I_{Vs}), and the fraction of channels which undergo CDI (ModeCa). Data are generated utilizing the same pacing protocol as Fig. 6. In **Panel B** recovery from CDI is prevented ($\theta = 0$ and $\delta = 0$ in the simulation) while in **Panel C** recovery from VDI is prevented (all transition rates into and out of I_{Vf} and I_{Vs} are set to 0). In these simulations, recovery from CDI or VDI is prevented when the number of channels inactivated via that mechanism has reached a maximum ($t = 1040$ ms and $t = 1165$ ms, respectively). Note that in both cases the EAD is abolished. The inset in **Panel A** shows

Open-state residency during the EAD on a magnified scale. For identification of the channel states, refer to Paper Fig. 1B.

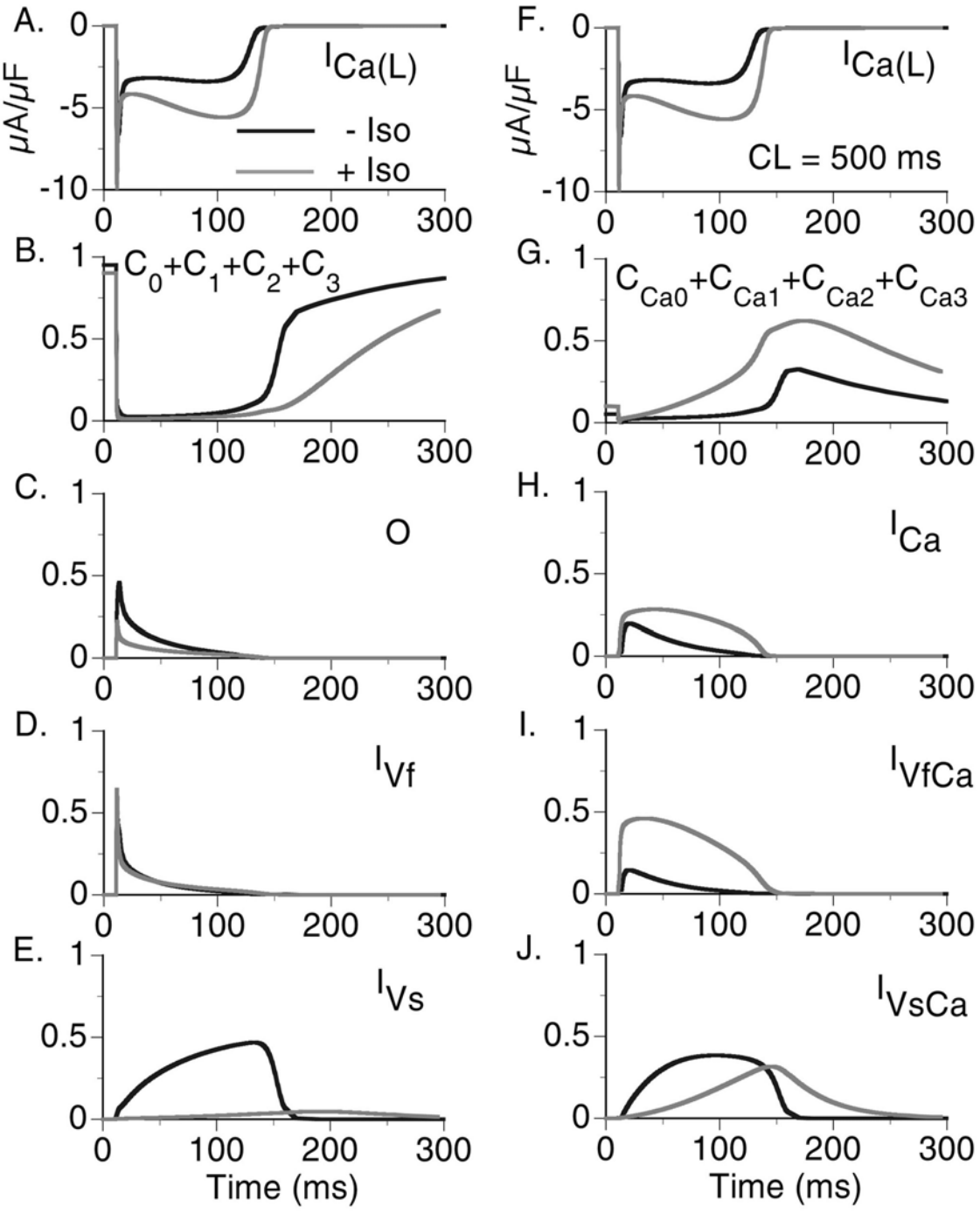
A.
$I_{Ca(L)}$
- Iso
+ Iso
μA/μF
B.
$C_0+C_1+C_2+C_3$
C.
O
D.
I_{Vf}
E.
I_{Vs}
F.
$I_{Ca(L)}$
CL = 500 ms
G.
$C_{Ca0}+C_{Ca1}+C_{Ca2}+C_{Ca3}$
H.
I_{Ca}
I.
I_{VfCa}
J.
I_{VsCa}
Time (ms)

Fig. E1

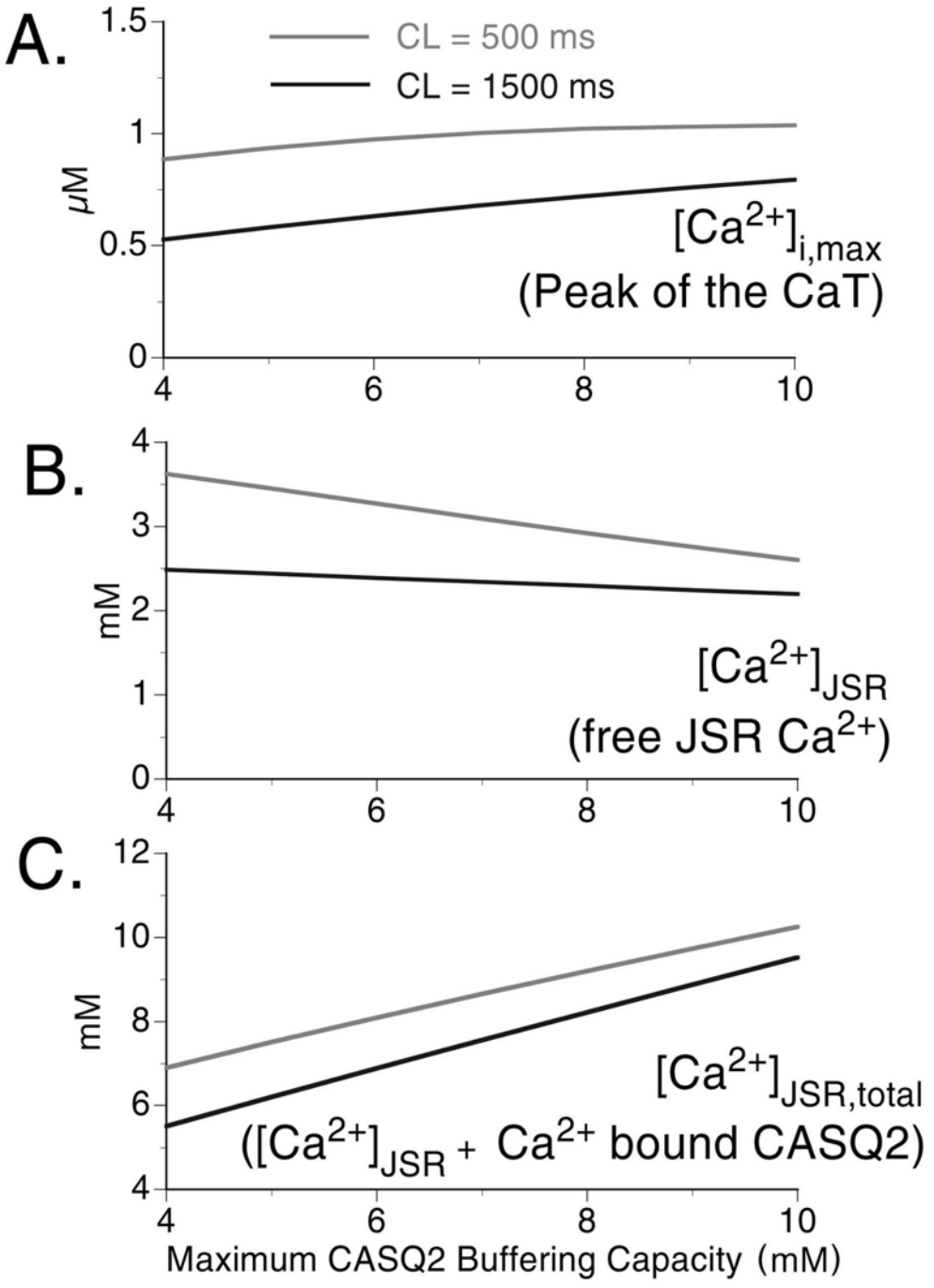
A.
CL = 500 ms
CL = 1500 ms
μM
1.5
1
0.5
0
$[Ca^{2+}]_{i,max}$
(Peak of the CaT)
B.
mM
4
3
2
1
0
$[Ca^{2+}]_{JSR}$
(free JSR Ca^{2+})
C.
mM
12
10
8
6
4
$[Ca^{2+}]_{JSR,total}$
($[Ca^{2+}]_{JSR}$ + Ca^{2+} bound CASQ2)
4
6
8
10
Maximum CASQ2 Buffering Capacity (mM)

Fig. E2

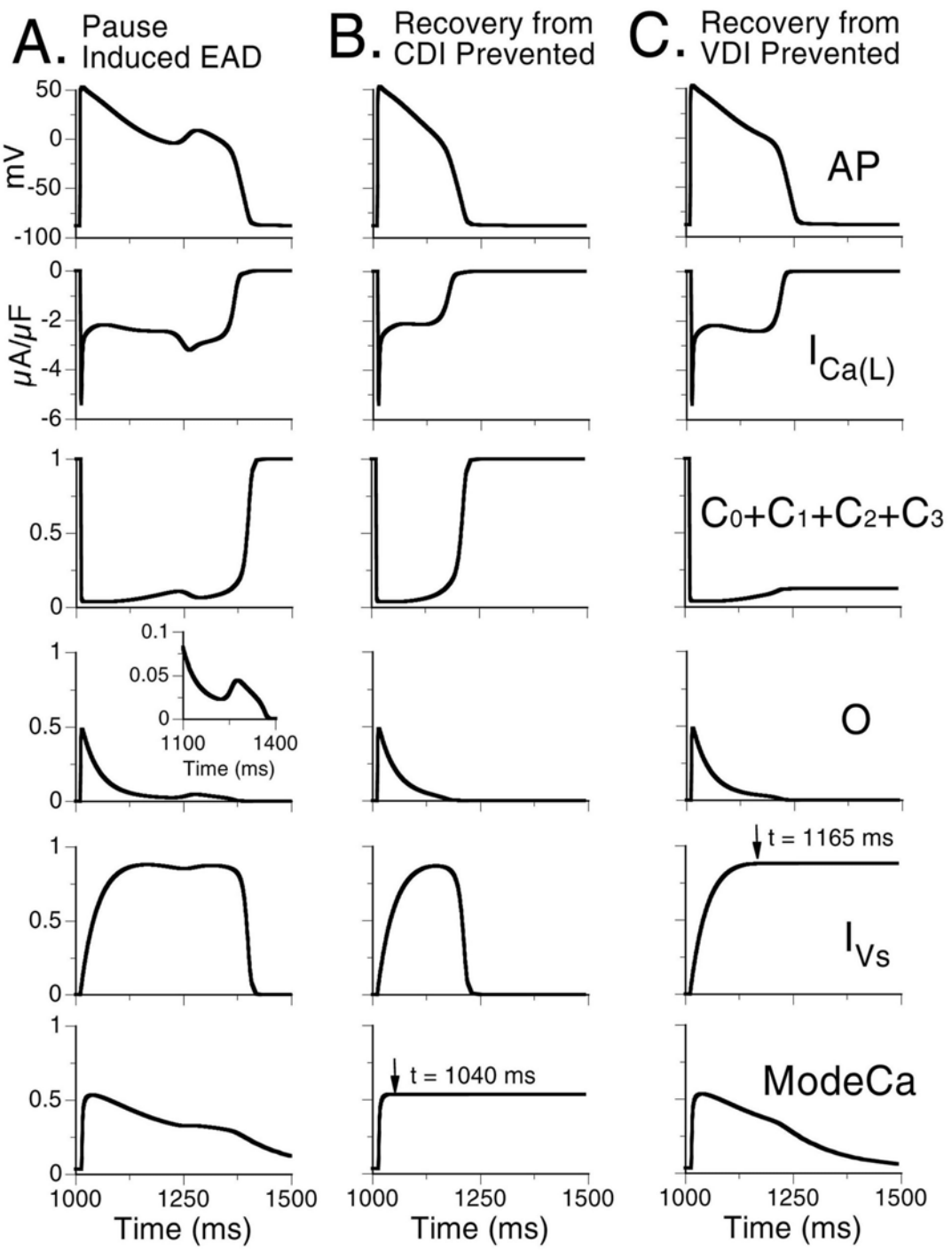
A. Pause Induced EAD
B. Recovery from CDI Prevented
C. Recovery from VDI Prevented
mV
AP
μA/μF
$I_{Ca(L)}$
$C_0+C_1+C_2+C_3$
O
t = 1165 ms
I_{Vs}
t = 1040 ms
ModeCa
Time (ms)
Time (ms)
Time (ms)

Fig. E3